Supporting Information:

Lithiation Confined in One Dimensional Nanospace of TiO_2 (Anatase) Nanotube to Enhance the Lithium Storage Property of CuO Nanowires

Ang Li; Huaihe Song; Xiaohong Chen; Jisheng Zhou; Zhaokun Ma*

State Key Laboratory of Chemical Resource Engineering; Beijing Key Laboratory of Electrochemical Process and Technology for Materials; Beijing University of Chemical Technology; Beijing; 100029; P.R. China.

AUTHOR INFORMATION

Corresponding Author

* E-mail: songhh@mail.buct.edu.cn; Fax: +86 10-64434916; Tel: +86 10-64434916

SI-1. XPS spectra analysis of $CuO@TiO_2$-NCAs

XPS spectra of $CuO@TiO_2$-NCAs are shown in Fig.S1. The curve fitting of Cu 2p, O 1s, and Ti 2p was carried out by using Gaussian-Lorentzian peak shape after a Shirley back-ground correction. In Fig. S1a, the Cu $2p_{3/2}$ peak is composed of two components at 931.8 and 933.9 eV, corresponding to Cu_2O and CuO, respectively.[s1,s2] The peaks at 529.9 and 531.5 eV can be assigned to oxygen bonded to Ti^{4+} and Ti^{3+}, as illustrated in Fig. S1b.[s3-s5] Binding energy positions of Ti $2p_{3/2}$ and Ti $2p_{1/2}$ for $CuO@TiO_2$-NCAs were 458.7 and 464.3 eV (Fig. S1c), respectively. These values are in good agreement with the binding energy values of Ti^{4+} in TiO_2. XPS spectra can also help to confirm the Ti^{3+} defects on the interfaces. The Ti^{3+} defects in anatase will destroy the symmetry of coordinated Ti^{4+} ions peak at 458.7 eV.[s6] A small shoulder at around 457.5 eV is consistent with the existence of Ti^{3+} defects on the interfaces, as can be seen in the red circle in Fig. S1d.[s6]

.

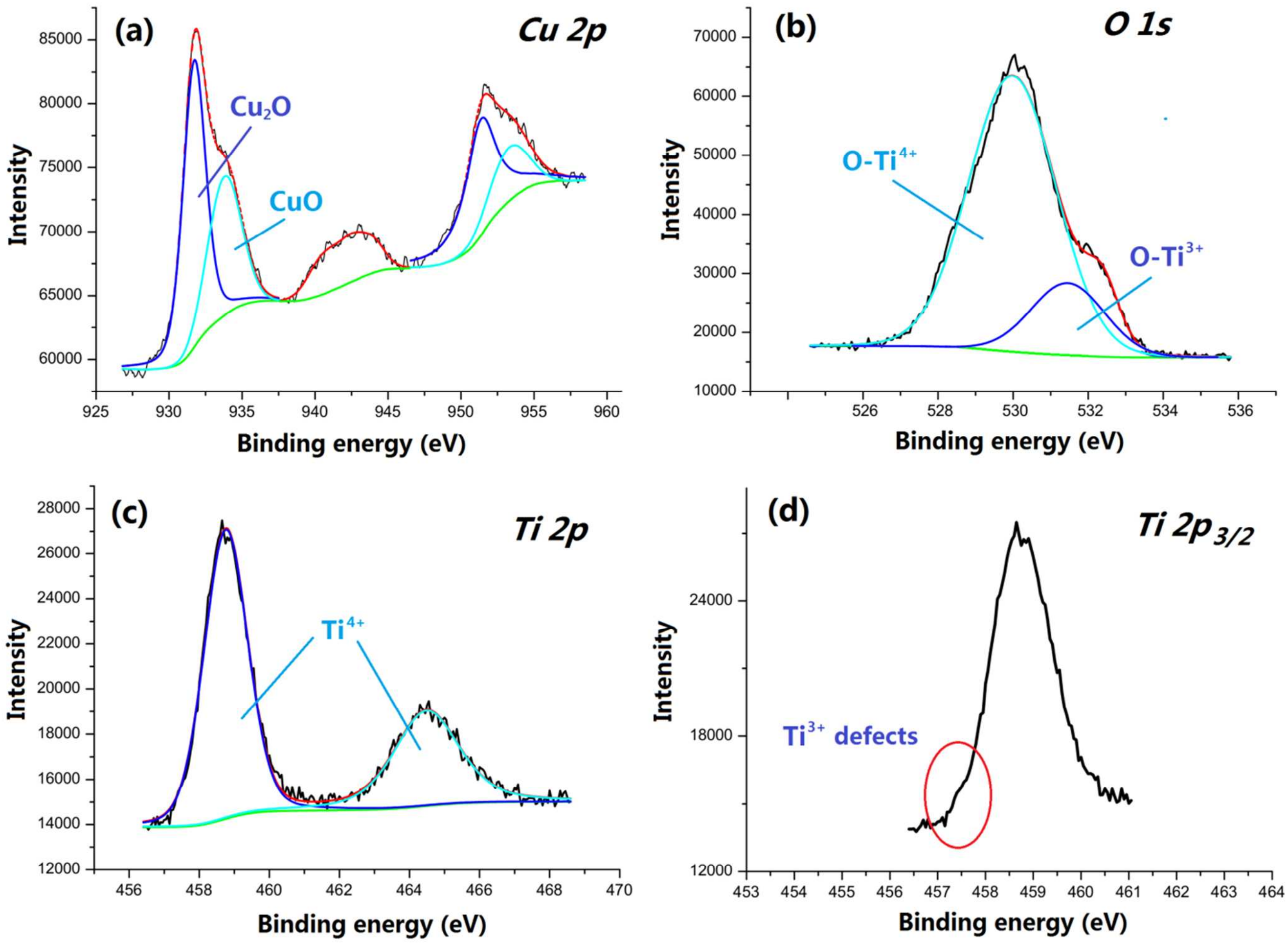

Fig.S1 XPS spectra of CuO@TiO_2-NCAs: (a)Cu2p; (b)O1s; (c)Ti2p; (d)Ti2p$_{3/2}$.

SI-2. Cyclic voltammograms of CuO@TiO_2-NCAs

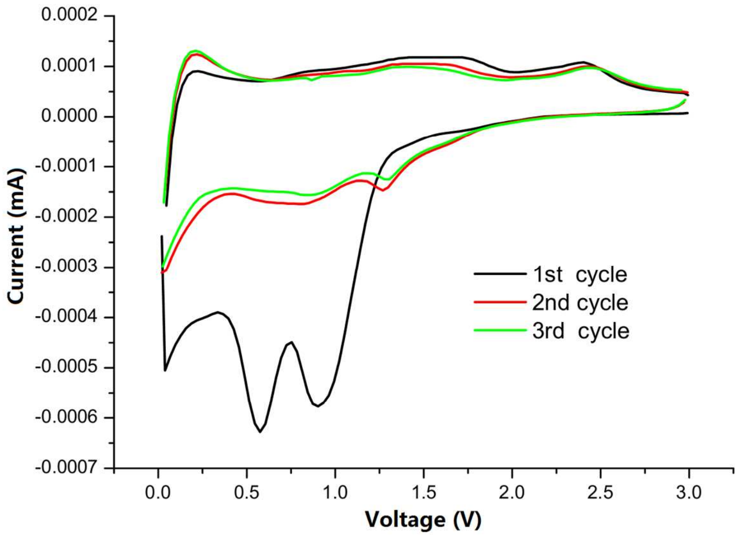

Fig.S2 Cyclic voltammograms of CuO-NWAs electrodes with scanning rate at 0.01 mV s^{-1} in the range of 0.01-3.0 V.

SI-3. Cycle performance of pure TiO_2

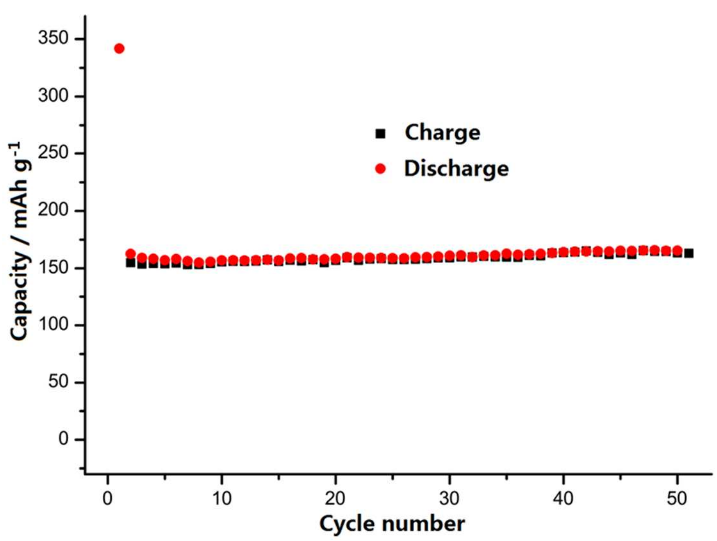

Fig.S3 The cycle performance of pure TiO_2 at 60 mA g^{-1} for 50 cycles.

SI-4. AC impedance spectra of CuO-NWAs

The AC impedance spectra of CuO-NWAs also used modified Randles equivalent circuit as the model for EIS analysis to quantify the experimental results. The results show that R_f and R_{ct} of CuO-NWAs is 9.25 and 40.26 Ω, respectively.

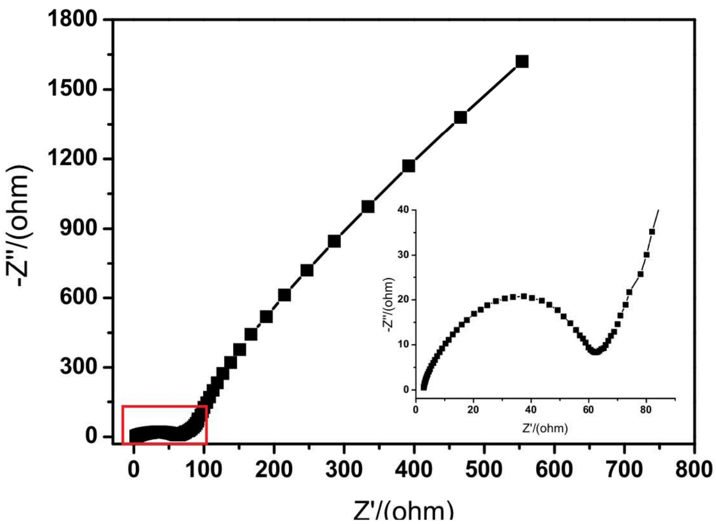

Fig.S4 AC impedance spectra of CuO-NWAs electrodes after 100 cycles (the inset is the part of the Nyquist plots in red box).

SI-5. HRTEM images of the CuO core in fully lithium insertion state

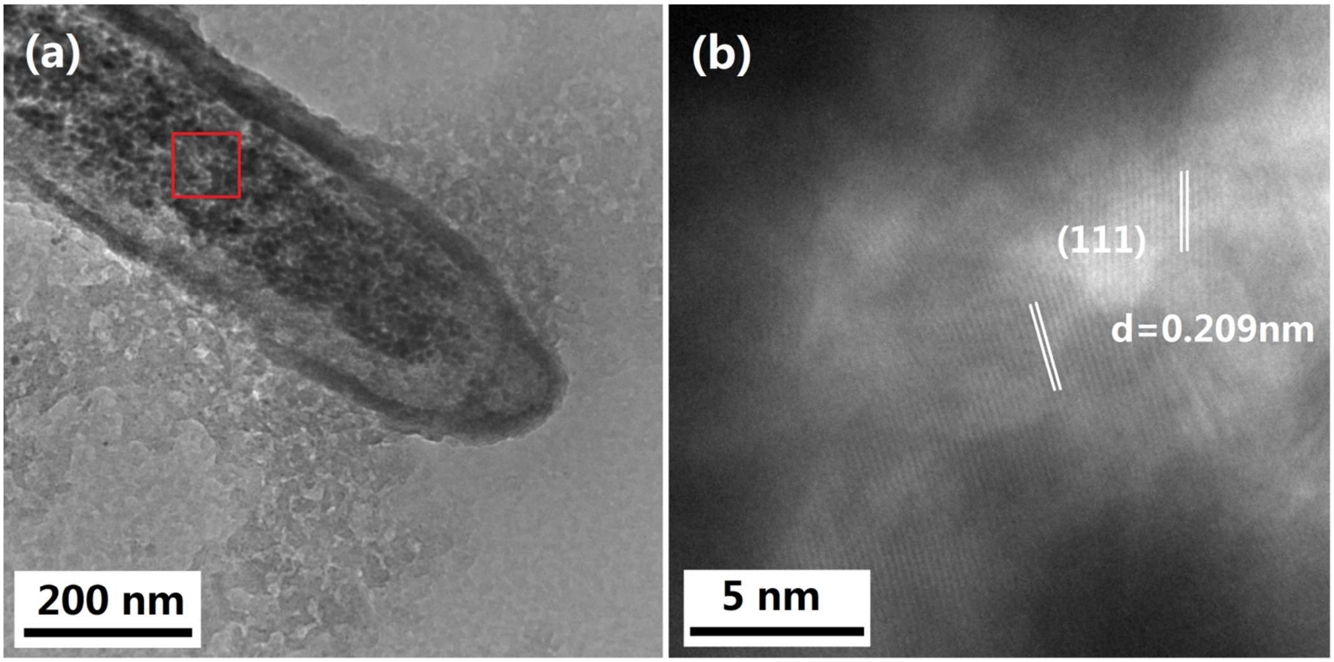

Fig.S5 HRTEM images of the CuO core in fully lithium insertion state: (a) a view of CuO@TiO_2-nanocable and its (b) details of the core.

References

(s1) Espinos, J.; Morales, J.; Barranco, A.; Caballero, A.; Holgado, J.; Gonzalez-Elipe, A. Interface Effects for Cu, CuO, and Cu_2O Deposited on SiO_2 and ZrO_2. XPS Determination of The Valence State of Copper in Cu/SiO_2 and Cu/ZrO_2 Catalysts. *J. Phys. Chem. B* **2002**, *106*, 6921-6929.

(s2) Poulston, S.; Parlett, P.; Stone, P.; Bowker, M. Surface Oxidation and Reduction of CuO and Cu_2O Studied Using XPS and XAES. *Surf. Interface Anal.* **1996**, *24*, 811- 820.

(s3) Kumar, P.; Badrinarayanan, S.; Sastry, M. Nanocrystalline TiO_2 Studied by Optical, FTIR and X-ray Photoelectron Spectroscopy: Correlation to Presence of Surface States. *Thin Solid Films* **2000**, *358*, 122–130.

(s4) Sharma, S.; Chaudhary, S.; Kashyap, S.; Sharma, S. Room Temperature Ferromagnetism in Mn Doped TiO_2 Thin Films: Electronic Structure and Raman Investigations. *J. Appl. Phys.* **2011**, *109*, 083905.

(s5) Orendorz, A.; Wüsten, J.; Ziegler, C.; Gnaser, H. Photoelectron Spectroscopy of Nanocrystalline Anatase TiO_2 Films. *Appl. Surf. Sci.* **2005**, *252*, 85–88.

(s6) Shultz, A.; Jang, W.; Hetherington III, W.; Baer, D.; Wang, L.; Engelhard, M. Comparative Second Harmonic Generation and X-ray Photoelectron Spectroscopy Studies of the UV Creation and O_2 Healing of Ti^{3+} Defects on (110) Rutile TiO_2 Surfaces. *Surf. Sci.* **1995**, *339*, 114–124.